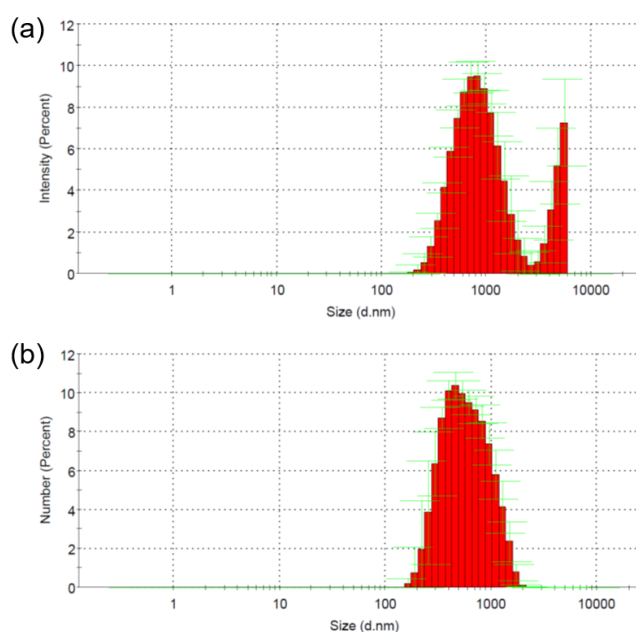


# Supplementary Materials

## Interpretation of DLS Result

On the basis of the result of DLS, as shown in Figure 2e in the main text, the intensity distribution (Figure S1a) can be converted into number distribution (Figures S1b). As several large flakes can be seen in the OM image (Figure 2a in the main text), such large flakes contributed to the peak at approximately 5000 nm in Figure S1a (Figure 2e in the main text). However, the number of such large flakes is negligible as depicted in Figure S1b. This is due to the principle of DLS, which is more sensitive to large particles than to small particles. Thus, the majority of the GO flakes is about the size of 100 to 1000 nm in diameter.



**Figure 1.** Results of DLS analysis. **(a)** Intensity distribution and **(b)** number distribution.

## Surface Profiles of GO and rGO Coatings on Si Substrates

To estimate the thickness of the GO layer coating MSS, we coated a silicon substrate with GO using the same inkjet process and measured its surface profile. The results are shown in Figure S2. While the GO layer is not uniform, its thickness is  $\sim 0.1 \mu\text{m}$ .

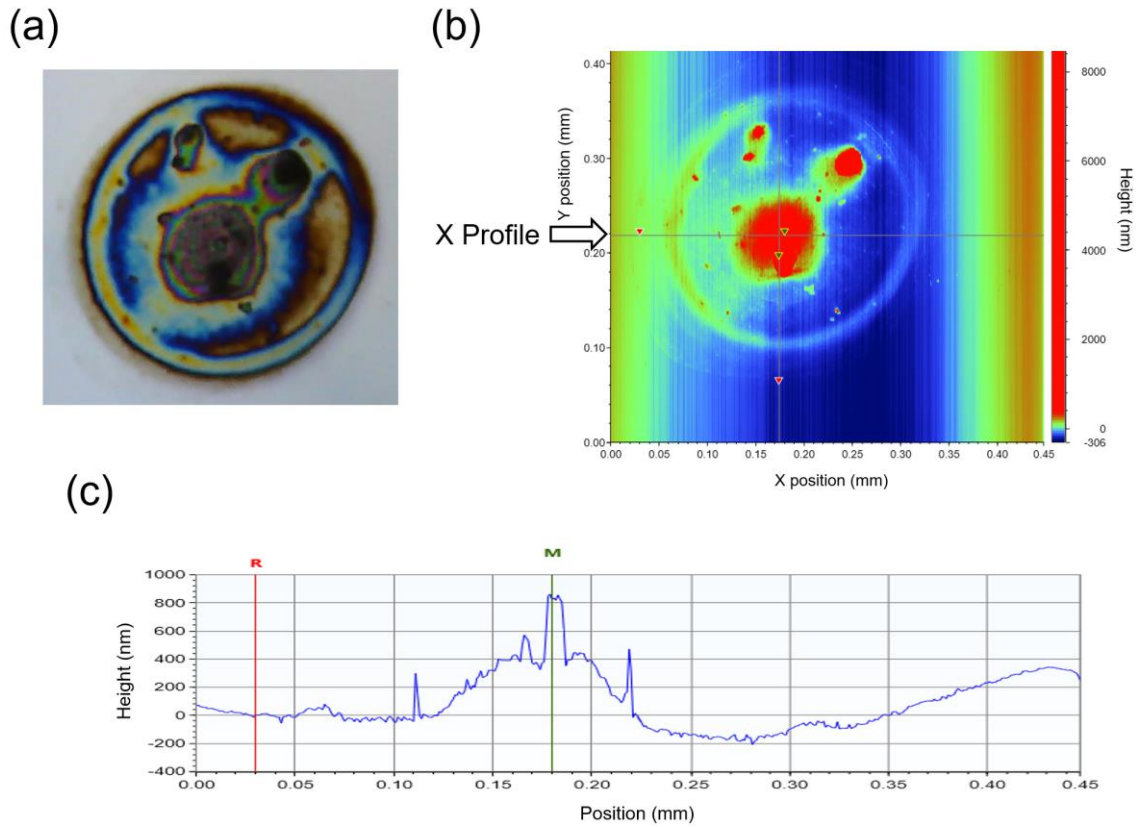


**Figure S2.** Surface profile of GO coating on Si Substrate. (a) Optical microscope image of the GO coating on a Si substrate. (b) Surface profile of GO. (c) Profile along the line indicated in (b).

A Si substrate was coated with the GO suspension using a micropipette to form a thick GO coating; 1  $\mu\text{L}$  of the GO suspension was applied to the Si substrate 10 times. The surface profile of the GO coating was obtained before and after vacuum annealing (Figure S3). After vacuum annealing, the thickness of the coating decreased from 0.4  $\mu\text{m}$  to 0.3  $\mu\text{m}$ .

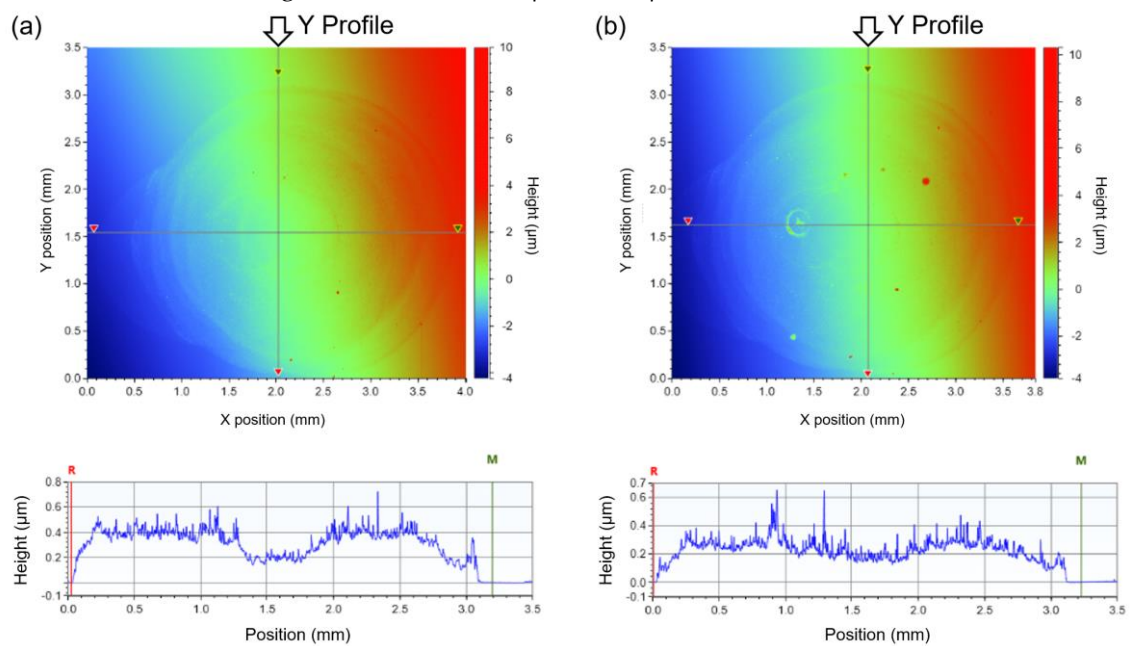


**Figure S3.** Effect of Vacuum annealing on Surface profile. Surface profiles of the GO-coated Si substrate (a) before and (b) after vacuum annealing. The profiles are shown on the same line.

### Peak-Fitting Analysis of Raman Spectra

Peak-fitting analysis was performed on the Raman spectra. In the range from 1100 to 2000  $\text{cm}^{-1}$ , the spectra were fitted with two Lorentzian peaks for GO and rGO (Figure S4a,b). For the graphite powder, the spectrum was fitted with four Lorentzian peaks (Figure S4c). On the basis of the result of the fitting,  $I_D/I_G$  was calculated from the peak areas. Although the fitting procedure was consistent, the fitting curves cannot fully reproduce the original spectra (Figure S4a,b). Thus, the quantitative discussion based on the calculated  $I_D/I_G$  is not exact.

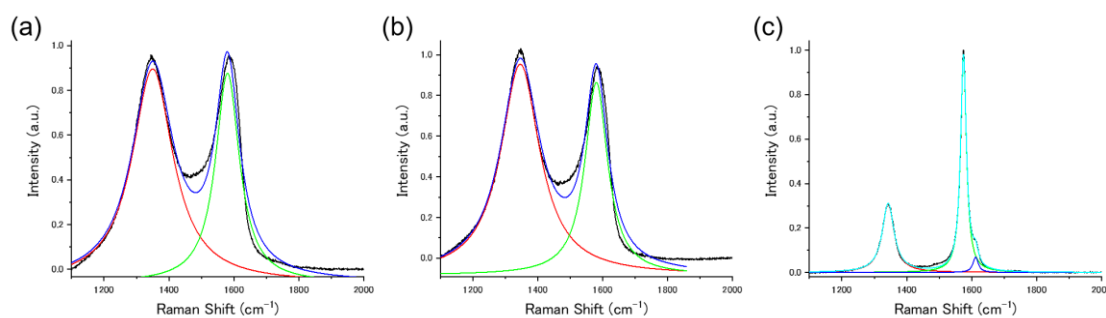


**Figure S4.** Peak Fitting Analysis on Raman Spectra. Results of peak fitting for (a) GO, (b) rGO, and (c) the graphite powder.

### Effects of the Drying Process

The experimental results showed that reduction of GO drastically decreased sensitivity (Figure 4 in the main text). In addition to the removal of oxygen-containing functional groups by thermal reduction, the loss of water retained in GO may have contributed to the decreased sensitivity, as Kim et al. reported that intercalated water enhances the absorption ability of GO [1]. To evaluate this effect, we prepared another GO-coated MSS and measured its sensing performance before and after the drying process. The GO-coated MSS was dried by annealing at 110  $^{\circ}\text{C}$  in a vacuum for 2 hours. As the results of thermogravimetric analysis (TGA) show that annealing at 110  $^{\circ}\text{C}$  can evaporate the water retained in GO without removing oxygen-containing functional groups (Figure 5 in the main text), MSS coated with dried GO can be obtained by the drying process.

Figure S5a shows the IR spectra of GO, GO annealed at 110  $^{\circ}\text{C}$  (dried GO), and GO annealed at 200  $^{\circ}\text{C}$  (rGO). The peaks assigned to oxygen-containing functional groups can be seen for GO and dried GO, while such peaks cannot be seen for rGO. Thus, GO is not reduced by the drying process. After the drying process, gas sensing measurement was quickly performed with the dried GO-coated MSS. Only heptane vapor was measured to avoid swelling of the dried GO with water vapor. The sensing signals before and after the drying process are shown in Figure S4b. After the drying process, the signal intensity decreases by approximately 40%.

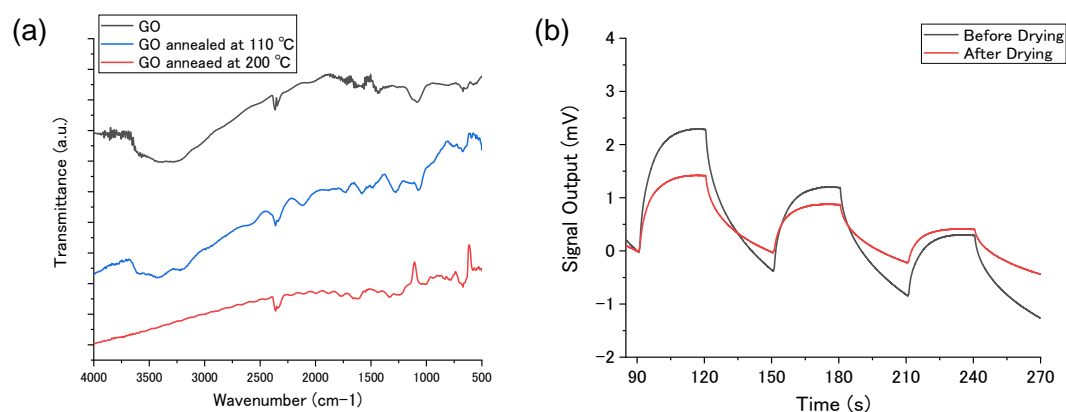


**Figure S5.** Properties of Dried GO. (a) IR spectra of GO, GO annealed at 110 °C (dried GO), and GO annealed at 200 °C (rGO). (b) Sensing signals of GO-coated MSS for heptane vapor before and after the drying process.

### Contribution of $V_a$ in the Sensing Model

Changes in  $d$ -spacing of GO laminates caused by gas sorption provides quantitative information related to the effects of  $V_a$ . Using neutron reflectivity, Klechikov et al. reported the  $d$ -spacing values of thin GO films exposed to solvent vapors as well as the number of absorbed molecules per formula unit [2]. According to the reported values, changes in  $d$ -spacing caused by 1 mol of gas molecules were calculated to be 3.4, 1.7, and 3.4 Å·f.u./mol for ethanol- $d_6$ ,  $D_2O$ , and acetone- $d_6$ , respectively. As widening of  $d$ -spacing is the main factor in expansion of GO, these values should be proportional to  $V_a$ . It is noteworthy that a deuterated water molecule does not significantly widen  $d$ -spacing. Rather, the water molecule caused smaller changes than did ethanol or acetone molecules. This seems inconsistent with the experimental results for the GO-coated MSS. However, such organic molecules cannot penetrate the  $\mu\text{m}$ -thick GO film, and the gas molecules can be absorbed only on the surface of the GO receptor layer, while water molecules can diffuse into the entire GO layer [3,4]. Thus, the total amount of absorbed molecules in the receptor layer should be higher for water than for the other gases, resulting in high sensitivity to water in spite of a low  $V_a$ .

### References

1. Kim, D.; Kim, D.W.; Lim, H.-K.; Jeon, J.; Kim, H.; Jung, H.-T.; Lee, H. Intercalation of Gas Molecules in Graphene Oxide Interlayer: The Role of Water. *J. Phys. Chem. C* **2014**, *118*, 11142–11148.
2. Klechikov, A.; Sun, J.; Vorobiev, A.; Talyzin, A. V. Swelling of Thin Graphene Oxide Films Studied by in Situ Neutron Reflectivity. *J. Phys. Chem. C* **2018**, *122*, 13106–13116.
3. Nair, R.R.; Wu, H.A.; Jayaram, P.N.; Grigorieva, I.V.; Geim, A.K. Unimpeded Permeation of Water Through Helium-Leak-Tight Graphene-Based Membranes. *Science* **2012**, *335*, 442–444.
4. Li, H.; Song, Z.; Zhang, X.; Huang, Y.; Li, S.; Mao, Y.; Ploehn, H.J.; Bao, Y.; Yu, M. Ultrathin, Molecular-Sieving Graphene Oxide Membranes for Selective Hydrogen Separation. *Science* **2013**, *342*, 95.